Sonic Band Gaps in Finite Elastic Media: Surface States and Localization Phenomena in Linear and Point Defects

M. Torres,[1] F. R. Montero de Espinosa,[2] D. García-Pablos,[3] and N. García[3]
[1]*Instituto de Física Aplicada, Consejo Superior de Investigaciones Científicas, Serrano 144, 28006 Madrid, Spain*
[2]*Instituto de Acústica, Consejo Superior de Investigaciones Científicas, Serrano 144, 28006 Madrid, Spain*
[3]*Laboratorio de Física de Sistemas Pequeños y Nanotecnología, Consejo Superior de Investigaciones Científicas, Serrano 144, 28006 Madrid, Spain*
(Received 21 September 1998)

The existence of surface states for sonic propagation in elastic band gap finite periodic systems is shown in this Letter. These surface states slide and propagate the sound along the surface edges as whispering galleries. We also experimentally observe such surface modes as well as localization phenomena in linear and point defects. [S0031-9007(99)08907-3]

PACS numbers: 43.35.+d

Photonic band gap structures have been widely studied in recent years [1–4]. A solid material that is transparent to a radiation may turn opaque, for some forbidden frequencies, by the appropriate modulation of the refraction index in the material. Such modulation creates band gaps for the propagation of modes (waves) inside the material and is analogous to Bragg reflections of electrons in solids [5]. In case of photonic crystals, bulk localized states have been predicted and observed [6,7] as well as states localized at the surface (surface states) have been calculated [8]. For elastic band gap materials, there are a large number of calculations for infinite periodic systems predicting gaps [9–13]. Moreover, the existence of full band gaps for ultrasonic propagation of waves in an Al matrix filled up with Hg cylinders has been recently demonstrated [14]. In this paper we show that surface state solutions are consubstantial with finite systems and exist for sonic propagation in finite elastic media. We also deal with several realizations of structures for ultrasonic propagation in elastic media to observe such surface state modes and localization phenomena in linear and point defects.

The wavelengths involved in elastic media when propagating ultrasounds (US) are in the range of millimeters. This implies that the modulations in elastic moduli needed to produce band gaps and related effects, when Bragg reflections are produced, are in the millimeter scale. Therefore, the involved technology consists of producing simply millimeter details in the sample matrix. Recently, by drilling millimeter cylinders filled up with Hg in an Al matrix, the existence of directional band gaps along the (100) and (110) directions, at the X and M symmetry points, has been shown, as well as a full band gap has been detected [14]. This gap is in good agreement with theoretical calculations [13]. Directional attenuation lengths were also measured. For elastic media, there is a reasonable amount of calculations for infinite systems [9–13]. However, systems are not infinite and there are boundaries for metal-vacuum or air (for US vacuum or air does not matter given the large impedance mismatch between media). Therefore, under a proper choice of parameters, states sliding and propagating along the surface and localized in the normal to the surface, i.e., surface states, should appear. These are analogous to electronic surface states in crystals [5] and to those calculated for photonic systems [8].

We proceed by describing the theory and equation governing the problem of the wave solutions at boundary surfaces. The equation for elastic waves in inhomogeneous solids [9–13,15] is

$$\frac{\partial^2 u_j^i}{\partial t^2} = \frac{1}{\rho_j}\left\{\frac{\partial}{\partial x_i}\left(\lambda_j \frac{\partial u_j^l}{\partial x_l}\right) + \frac{\partial}{\partial x_l}\left[\mu_j\left(\frac{\partial u_j^i}{\partial x_l} + \frac{\partial u_j^l}{\partial x_i}\right)\right]\right\}, \quad (1)$$

where u_j^i is the ith component of the displacement vector $\mathbf{u}(\mathbf{r})$, $\lambda(\mathbf{r})$, and $\mu(\mathbf{r})$ are the so-called Lamé coefficients, $\rho(\mathbf{r})$ is the density, and j describes the medium: air $j = 1$, elastic media $j = 2$.

The longitudinal and transverse velocities for the homogenous case ($\lambda, \mu, \rho = \text{const}$) are given by

$$c_l = \sqrt{\frac{\lambda + 2\mu}{\rho}}, \qquad c_t = \sqrt{\frac{\mu}{\rho}}. \quad (2)$$

For fluids, $\mu = 0$, and Eq. (1) becomes

$$\frac{\partial^2 p}{\partial t^2} = \lambda \nabla\left(\frac{\nabla p}{\rho}\right) \quad (3)$$

by introducing the pressure $p = -\lambda \nabla u$.

Band structure and band gaps appear when $\lambda(\mathbf{r})$, $\mu(\mathbf{r})$, and $\rho(\mathbf{r})$ vary periodically in the elastic media. However, at the band gaps, surface states appear when boundary conditions are imposed at the points $\mathbf{r}_s$ describing the interface air-elastic media. These boundary conditions state the continuity of the displacements

$$u_1^i(\mathbf{r}_s) = u_2^i(\mathbf{r}_s) \quad (4)$$

and the continuity of the integral of Eq. (1) along the

 0031-9007/99/82(15)/3054(4)$15.00

interface $\mathbf{r}_s$, giving

$$\lambda_1 \frac{\partial u_1^l}{\partial x^l} + 2\mu_1 \frac{\partial u_1^1}{\partial x_1} = \lambda_2 \frac{\partial u_2^l}{\partial x^l} + 2\mu_2 \frac{\partial u_2^1}{\partial x_1}, \qquad \mu_1\left(\frac{\partial u_1^2}{\partial x_1} + \frac{\partial u_1^1}{\partial x_2}\right) = \mu_2\left(\frac{\partial u_2^2}{\partial x_1} + \frac{\partial u_2^1}{\partial x_2}\right), \tag{5a}$$

where $i = 1, 2$ and $(x_1, x_2) = (x, y)$ for a 2D system.

Notice that for fluids, $\mu = 0$, and if $\lambda_1 \ll \lambda_2$, case of air metal, then Eq. (5a) becomes

$$\frac{\partial u_2^l}{\partial x^l} \approx 0. \tag{5b}$$

By Fourier transforming Eq. (1), one obtains the secular equation linking the frequencies ω to the reciprocal vectors G that by Floquet-Bloch's theorem defines the band structure in elastic media [9–13].

The boundary conditions (4) and (5) along with Eq. (1) provide solutions that are localized at the interfaces and propagate along them.

We have solved these equations, for the case $\mu = 0$, in 2D and found the surface states localized in k_x and propagating in k_y for values of the wave vector $k_x = -[G(0,1)/2] + i\delta$ describing the Bragg reflection $(G/2)$, with the localization length given by δ^{-1} and $k_y \ll G(1,0)/2$ (see Ref. [16]). It reads

$$u_x = Ae^{-\delta x}\cos\left(\frac{G}{2}x + \phi\right)e^{ik_y y}, \tag{6}$$

where $\delta(\omega)$ and $\phi(\omega)$ are defined by the boundary conditions (5) and A is a normalization constant. Figure 1(a) shows the band structure for air cylinders immersed in water with a filling factor $f = 0.3$, which means that 30% of the volume is air. The bands are for the Γ-X and Γ-M directions. Figure 1(b) shows the surface states that satisfy boundary conditions located at $\mathbf{r}_s(x_0, y)$ as sweeping the unit cell. There is a surface state for each x_0 at the X symmetry point. This state develops in a band as k_y increases from 0 to $G(1,0)/2$. Analogously, by symmetry, there are surface states localized in y and propagating in x for the boundary $\mathbf{r}_s(x, y_0)$ and described by the same solution (6), where $x \rightarrow y$ and $k_x \rightarrow k_y$ and vice versa. The inset of Fig. 1(b) shows the region populated by surface states with decay length δ^{-1}. The maximum δ is related to the band gap width. The larger the band gap width, the larger the maximum δ. For the sake of simplicity, we have presented results for $\mu = 0$. However, the same result should hold for the most general case $\mu \neq 0$ as has been discussed in laminar composites [17].

In order to prove experimentally the above results, we have used the Al-Hg composite samples previously described [14]. The specific acoustic impedance of both Al host and Hg scatterers are 18.2×10^6 and 19.7×10^6 kg m^{-2} s^{-1}, respectively. Thus, the contrast in acoustic impedance is small. Band gaps appear even though there is not a strong impedance contrast. We have coupled an US piezoelectric transducer to the sample as indicated in the inset of Fig. 2, launching a monochromatic wave at the frequency of 0.75 MHz, in the middle of the strong directional gap along the (100) direction. The vibration amplitude of the elastic waves were scanned at the x-y surface of the sample by means of a broadband needle hydrophone coupled to the sample by a thin layer of a coupling liquid, as described elsewhere [14]. In this case, a surface state should be localized in the y direction and propagating in the x direction. As discussed above, by symmetry, other surface states exist propagating in y and localized in x [see inset of Fig. 1(b)]. Because of the small size of the transducer, it also produces waves propagating along y that, at gap frequencies, should localize in x. Figure 2 shows the amplitude record of an Al-Hg composite plate with a 40% mercury filling ratio, with the diameter of the cylinders of 2 mm and the unit cell length $a = 2.8$ mm. The scanned surface is 15×23 mm^2. The width, in the x direction, of the exciting transducer surface is 5 mm. The distance from the plate plane boundary to the centers of the first mercury cylinder row is 3 mm.

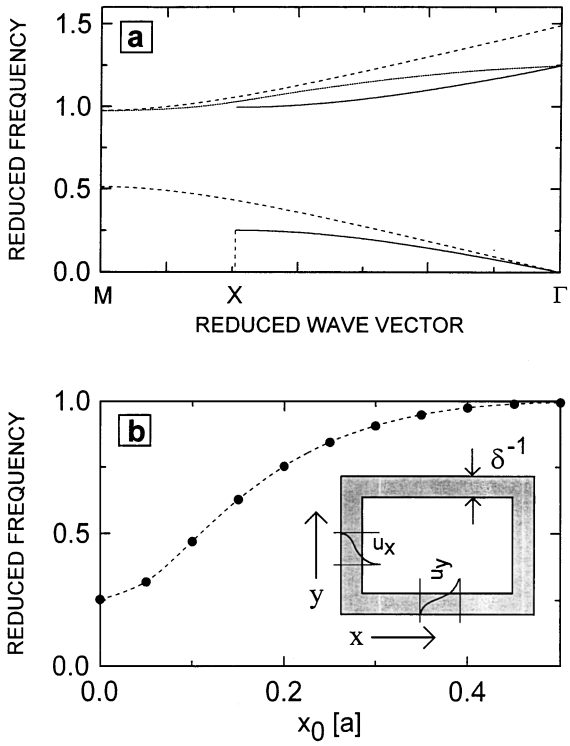

FIG. 1. (a) Shows the band structure for air cylinders immersed in water along the Γ-X and Γ-M directions. It is shown that a big full band gap exists in agreement with previous calculations [10]. In (b) we present the surface states at the X point that satisfy the boundary conditions (4) and (5a) at x_0: in this case both of them are equivalent to (5b). The inset shows the localization of the surface states around elastic media with the schematic decay of the displacements u_x and u_y that extend in the fringe δ^{-1}.

The recorded amplitude signal (Fig. 2), measured along x and y at the interfaces, shows a clear propagation along

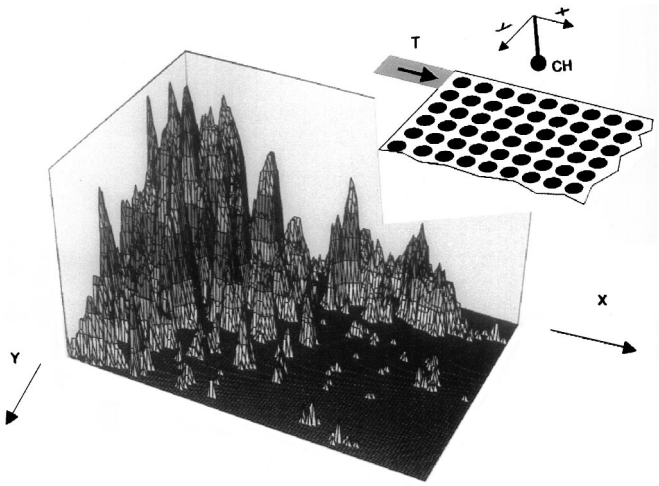

FIG. 2. A 3D contour plot of the surface amplitude scan of the metallic composite of the inset when a monochromatic excitation wave of 0.75 MHz was launched from one corner of the sample. Notice the appearance of clear surface states along the boundaries and a week penetration along the (110) direction. This last weak propagation appears because, at the excitation frequency, the attenuation along the (110) direction is less than along the (100) direction. The inset indicates the corresponding geometry and the coupled hydrophone (CH).

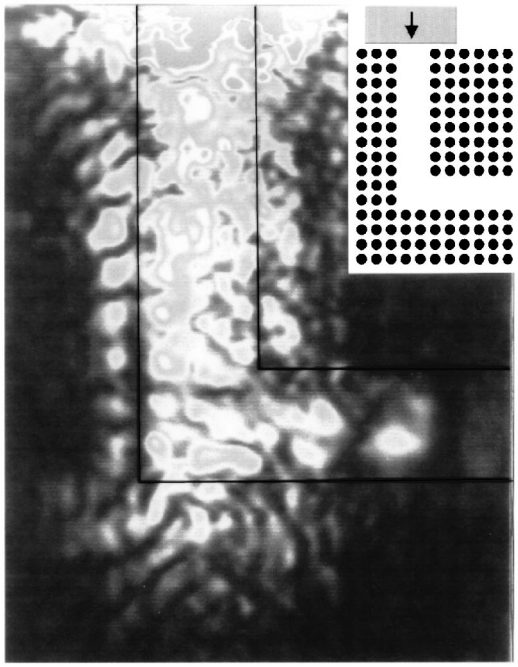

FIG. 3. Surface amplitude scan of a metallic composite with an L-shaped linear defect. The excitation frequency is 0.75 MHz. Note that the radiation is guided along the path free of holes (superimposed lines indicate the path free of holes). The lateral penetration along the (010) direction affects only the first row of cylinders. At the corner of the L-shaped path the radiation comes slightly in the composite along the $(1, 1, 0)$ and $(1, -1, 0)$ directions. The inset shows the geometry and the transducer position.

lateral surfaces. The signal amplitude is larger at the interfaces and dies off exponentially in the elastic media. The decay length is larger in the (110) direction than in the (100) direction, in agreement with δ values: $\delta_{100}^{-1} \approx 2a$, $\delta_{110}^{-1} \approx 3.5a$, as measured. The reason we used Hg cylinders in Al matrix is not only for scientific convenience but also to have the signal always contained in the elastic sample. No transmission to surrounding air exists because of the large mismatch of elastic moduli [17]. This would permit directing sound and US and redistributing sonic signals. Recent experiments about sound gaps [18] have found directional gaps that would also be enough to slide the sound along the surface of the studied structure.

On the other hand, as an example of a linear defect, in Fig. 3 we present the propagation of US when two rows of Hg cylinders are missing according to an L-shaped structure (see inset of Fig. 3). A monochromatic 0.75 MHz excitation signal, corresponding to the center of the band gap along the (100) main symmetry direction, was launched along the missed rows scanning the vibration amplitude at the x-y surface of the sample. The active

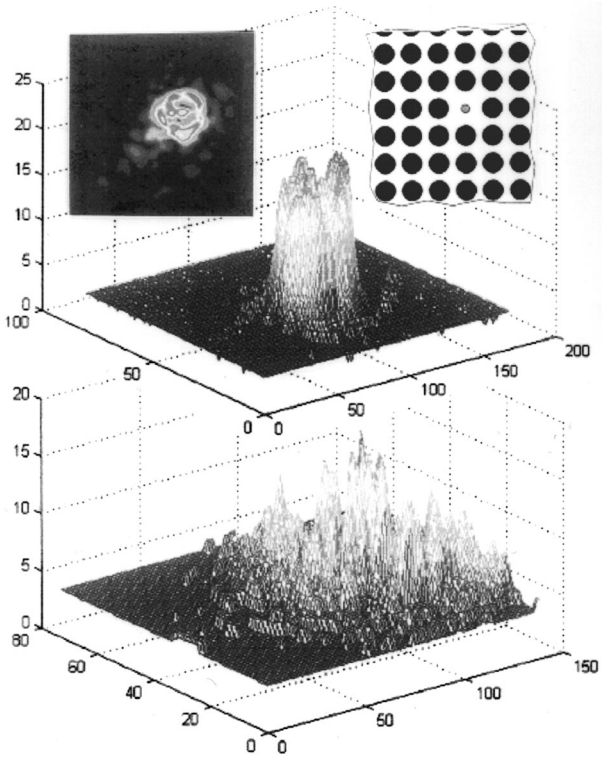

FIG. 4. A 3D contour plot of the surface amplitude scan of a metallic composite with a point defect. A cylinder has been substituted by a piezoelectric vibrator excited at a frequency of 0.75 MHz. Note the strong localization of the wave (top). The left inset is the direct surface amplitude scan. The right inset indicates the vibrator position in the lattice. A 3D contour plot of a surface amplitude scan when the vibrator excites the sample at a frequency of 1.3 MHz, clearly out of the gap, is shown at the bottom of the figure. Note the expected spreading of the ultrasonic wave in this case.

aperture of the transducer is 3 times the width of the path free of holes. In this experiment, the radiation is guided along the path free of holes and is able to illuminate the right arm of the L-shaped path.

We have also dealt with localized states. With this aim, we have substituted one Hg cylinder by a piezoelectric vibrator that we have excited at a frequency of 0.75 MHz, within the band gap, and at 1.3 MHz, clearly outside the gap. Scans of the vibration amplitude at the x-y surface sample were performed. Results are presented in Fig. 4. In the first case, the frequency is in the middle of the gap. Consequently, the localization of the wave strongly appears. See Fig. 4 (top) and its insets. The wave localization at frequencies in the center of the full gap is isotropic. As far as the frequency is increased up to the edge of the full band gap, the exponential decaying length linearly increases. At a wave frequency far away from the gaps, as it is expected, the wave is completely delocalized spreading out (Fig. 4, bottom). This experimental setup can also be used to study in detail unsettled questions of classical wave localization in 2D random systems.

This work has been supported by DGICYT, CICYT, and ESPRIT EU projects. We thank Professor A. P. Levanyuk for discussions.

[1] E. Yablonovitch, Phys. Rev. Lett. **58**, 2059 (1987).
[2] S. John, Phys. Rev. Lett. **58**, 2486 (1987).
[3] C. M. Soukoulis, *Photonic Band Gaps and Localization*, NATO ASI, Ser. B, Vol. 308 (Plenum, New York, 1993); K. M. Ho, C. T. Chan, and C. M. Soukoulis, Phys. Rev. Lett. **65**, 3152 (1990); K. M. Leung and Y. F. Liu, Phys. Rev. Lett. **65**, 2646 (1990); M. M. Sigalas, E. N. Economou, and M. Kafesaki, Phys. Rev. B **50**, 3393 (1994).
[4] *Scattering and Localization of Classical Waves in Random Media*, edited by P. Sheng (World Scientific, Singapore, 1990).
[5] C. Kittel, *Introduction to Solid State Physics* (Wiley, New York, 1971); A. Haug, *Theoretical Solid State Physics* (Pergamon Press, Oxford, 1972).
[6] R. D. Meade *et al.*, Phys. Rev. B **44**, 13 772 (1991).
[7] E. Yablonovitch *et al.*, Phys. Rev. Lett. **67**, 3380 (1991).
[8] R. D. Meade *et al.*, Phys. Rev. B **44**, 10 961 (1991).
[9] M. M. Sigalas and E. N. Economou, J. Sound Vib. **158**, 377 (1992); Solid State Commun. **86**, 141 (1993).
[10] E. N. Economou and M. M. Sigalas, Phys. Rev. B **48**, 13 434 (1993).
[11] M. M. Sigalas and E. N. Economou, Europhys. Lett. **36**, 241 (1996).
[12] M. S. Kushwaha *et al.*, Phys. Rev. Lett. **71**, 2022 (1993); M. S. Kushwaha *et al.*, Phys. Rev. B **49**, 2313 (1994).
[13] M. M. Sigalas (private communication); J. Appl. Phys. **84**, 3026 (1998).
[14] F. R. Montero de Espinosa, E. Jiménez, and M. Torres, Phys. Rev. Lett. **80**, 1208 (1998).
[15] L. D. Landau and E. M. Lifshitz, *Theory of Elasticity* (Pergamon Press, London, 1959).
[16] In this case, for simplicity and to illustrate the solution for surface states, we have approximated the Bragg reflection by the vector $k_x = -G/2$ and $G/2$.
[17] B. A. Auld, G. S. Beaupre, and G. S. Hermann, Electron. Lett. **13**, 525 (1997).
[18] J. V. Sánchez-Pérez *et al.*, Phys. Rev. Lett. **80**, 5325 (1998).